2019 International Conference on Optical MEMS and Nanophotonics
July 28 - August 1, 2019 / KAIST, Daejeon, Korea

Multi-functional Infrared Metamaterial Absorber

Ruijia Xu, Dongyuan Yao, Zefeng Xu, and Yu-Sheng Lin*
State Key Laboratory of Optoelectronic Materials and Technologies,
School of Electronics and Information Technology, Sun Yat-Sen University,
Guangzhou, China
linyoush@mail.sysu.edu.cn

***Abstract*—We propose four types of infrared metamaterial absorber (IRMA) to have tunable absorption resonance, polarization-dependent/independent, single-band and dual-band switch characteristics. To tailor four IRMAs with different height between top and bottom metal layers, absorption resonance can be modified 2.07 μm and absorption intensity can be attenuated gradually. These characteristics of IRMA can be potentially used in variable optical attenuator (VOA). By changing the distance between top unit cells of four IRMAs, the resonances can be tuned in the range of 1.74 μm with an exponential relationship. All absorption intensities can be kept as higher than 90%. This study provides a strategy to open an avenue for VOA, absorber, detector, sensor, and switch applications in IR wavelength range.**

Keywords—metamaterials, IR absorber, multi-functionalities

I. Introduction

Metamaterials are artificial materials that allow people to control the electromagnetic wave by properly tailoring. They are widely studied in many fields, such as cloaking devices, high-sensitive sensors, perfect absorbers, security screening, medical imaging, and non-destructive testing [1-3]. Among of metamaterial fields, infrared metamaterial absorber (IRMA) is one of the most important applications due to its flexibility and applicability in solar cells, thermal emitters and refractive index sensor, etc.

In this study, we propose four types of reconfigurable metamaterials on Si substrate to perform tunable IRMA. The top metamaterials are free-standing structures and exhibit flexible tunabilities by changing geometrical configurations of top metamaterials, i.e. modified the height between top and bottom metal layers and distance between top tailored metal layer. By modifying geometrical configurations of metamaterials, these four IRMA show different active and flexible tunabilities in absorption intensities and resonances. These results indicate our proposed IRMAs can be potentially used for absorber, detector, sensor, and switch applications.

II. Materials and Methods

Fig. 1 shows schematics of proposed IRMAs. They are metamaterials tailored with cross-shape (IRMA-1), I-shape (IRMA-2), T-shape (IRMA-3), and U-shape (IRMA-4) nanostructures, respectively. These nanostructures are top tailored Au layer, air, bottom Au layer, and Si substrate from top to bottom, respectively. The denotations of Fig. 1 are heights between top and bottom Au layers (H_1-H_4) and distances between top tailored Au layer (D_1-D_4). The subscript numbers of 1, 2, 3 and 4 are denoted as IRMA-1, IRMA-2, IRMA-3, and IRMA-4, respectively. All metal widths of top tailored Au layer are kept as constant as 1 μm.

III. Results and Discussions

Fig. 2(a) shows the absorption spectra of IRMA-1. It indicates that the absorption intensity gradually decreased from H_1 = 0.2 μm to H_1 = 1.4 μm. The maximum absorption intensity of IRMA-1 with H_1 = 0.2 μm is 97% in 12.85 μm wavelength, which will decay to 15% in 14.92 μm wavelength at the condition of H_1 = 1.4 μm. The tuning ranges of absorption resonance and absorption intensity are 2.07 μm and 82%, respectively. For the absorption resonances of IRMA-2, IRMA-3 and IRMA-4 are red-shifts and the bandwidths become broad, while the absorption intensity becomes lower gradually as shown in Fig. 2(b-d). It is clearly observed that there is perfect absorption for IRMA-2 with H_2 = 0.2 μm in 13.21 μm wavelength, which can greatly improve the performance of switch. As there is almost no absorption with metamaterial height more than 1.4 μm for the proposed designs. These results provide the potential opportunity for IR variable optical attenuator (VOA) application by changing the height of top and bottom Au layers.

By changing the distance between unit cell of top tailored Au layer of four IRMAs, the absorption spectra of IRMA-1, IRMA-2, IRMA-3, and IRMA-4 are shown in Fig. 3(a-1), Fig. 3(b-1), Fig. 3(c-1), and Fig. 3(d-1), respectively. There are three kinds of configurations of IRMA-1 by changing D_1 from 0 μm to 2.0 μm as shown in Fig. 3(a-2), Fig. 3(a-3), and Fig. 3(a-4), respectively. At the condition of D_1 = 0 μm, IRMA-1 is the configuration of cross-shape (Fig. 3(a-2)) and exhibits absorption resonance at 12.85 μm wavelength. When D_1 is increased to 0.1 μm, the configuration of IRMA-1 becomes T-bar-shape as shown in Fig. 3(a-3). The absorption resonance is shift to 11.76 μm wavelength. At the conditions of D_1 = 0.1 μm to 1.9 μm, IRMA-1 is maintained to keep as the configuration of T-bar-shape, the absorption resonance is red-shift from 11.76 μm to 12.56 μm wavelength and exhibits an exponential tunability as shown in Fig. 4(a). As D_1 increased to 2.0 μm, IRMA-1 is formed the configuration of T-shape as shown in Fig. 3(a-4). The absorption resonance is shift to 18.62 μm.

At the condition of D_2 = 0 μm, IRMA-2 is the configuration of I-shape (Fig. 3(b-2)), whose absorption resonance is at 13.21 μm wavelength. When D_2 is increased to 0.1 μm, IRMA-2 is the configuration of U-bar-shape as shown in Fig. 3(b-3). The absorption resonance is shift to 10.71 μm wavelength. At the conditions of D_2 = 0.1 μm to 1.9 μm, IRMA-2 is maintained to keep as the configuration of U-bar-shape, the absorption resonance is red-shift from 10.71 μm to 11.42 μm wavelength and exhibits an exponential tunability as shown in Fig. 4(b). As D_2 increased to 2.0 μm, IRMA-2 is formed the configuration of U-shape as shown in Fig. 3(b-4). The absorption resonance is at 16.42 μm wavelength. All resonances are perfect absorptions. Compared with IRMA-1, there are identical electromagnetic responses for IRMA-2 with D_2 less than 2.0 μm.

When the width of vertical bar of IRMA-1 becomes double, it is formed the shape of IRMA-3 as shown in Fig. 3(c-2). While D_3 is less than 0.9 μm, there is identical resonance shift for IRMA-3, as shown in Figs. 3(c-1) and 4(c). The maximum D_3 is 1.0 μm, which helps IRMA-3 to form the

978-1-7281-4503-7/19/$31.00 ©2019 IEEE

H-shape as shown in Fig. 3(c-4). It shows no absorption of incident light.

By using the same approach, the absorption resonance of IRMA-4 with D_4 = 0 μm is at 14.84 μm wavelength. The configuration is I-shape with double width of vertical bar as shown in Fig. 3(d-2). The resonance shift is identical with IRMA-1 and IRMA-2 as shown in Fig. 3(d-1) and 4(d). The absorption resonance is 22.2 μm wavelength. It can be concluded that all designs have three different configurations and each one shows great difference in absorption resonance. Such designs have tunabilities in absorption intensity and resonance. The maximum resonance shifts of IRMA-1, IRMA-2, IRMA-3 and IRMA-4 are 6.86 μm, 5.71 μm, 1.74 μm, and 10.64 μm, respectively. The proposed devices exhibit larger tunability of absorption resonance, which means that a larger resonance-shift can be achieved. Such designs are suitable for tunable IR absorber application.

IV. Conclusion

In conclusion, four IRMAs are proposed to perform multi-functional applications. The heights between top and bottom metal layers of proposed devices can be modified to tune the absorption intensity and resonance. The tuning range of absorption resonance can be reached 5 μm and absorption intensity can gradually attenuated. By changing the distance between top unit cells of IRMAs, their absorption resonances can be tuned to have an exponential relationship. The tuning ranges are spanned 6.86 μm, 5.71 μm, 1.74 μm, and 10.64 μm for IRMA-1, IRMA-2, IRMA-3, and IRMA-4, respectively. According to above mentioned, our proposed IRMAs can be used in widespread applications, such as sensor, absorber, detector, switch, VOA, and so on.

References

[1] Y. S. Lin, C. Y. Huang, and C. Lee, "Reconfiguration of Resonance Characteristics for Terahertz U-Shape Metamaterial Using MEMS Mechanism," *IEEE J. Sel. Top. Quantum Electron.*, vol. 21, pp. 2700207, 2015.

[2] N. I. Zheludev and Y. S. Kivshar, "From metamaterials to metadevices," *Nature Mater.*, vol. 11, pp. 917-924, 2012.

[3] Y. Zhang, T. Li, Q. Chen, H. Zhang, J. F. O'Hara, E. Abele, A. J. Taylor, H. T. Chen, and A. K. Azad, "Independently tunable dualband perfect absorber based on graphene at mid-infrared frequencies," *Sci. Rep.*, vol. 5, pp. 18463, 2015.

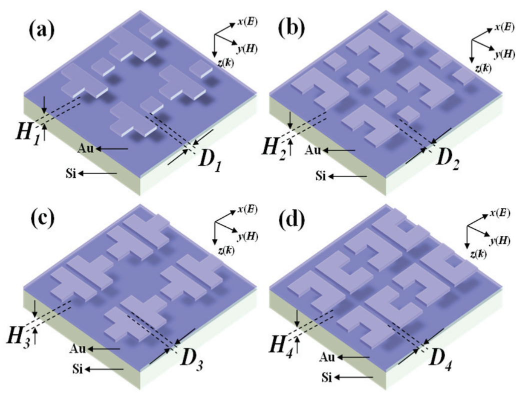

Fig. 1. Schematics of (a) IRMA-1, (b) IRMA-2, (c) IRMA-3 and (d) IRMA-4, respectively.

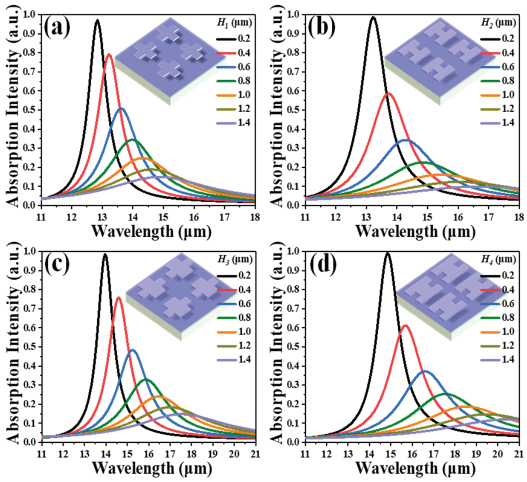

Fig. 2. Absorption intensities of (a) IRMA-1, (b) IRMA-2, (c) IRMA-3, and (d) IRMA-4 with different height between top and bottom Au layers, i.e. H_1, H_2, H_3, and H_4 for IRMA-1, IRMA-2, IRMA-3, and IRMA-4, respectively.

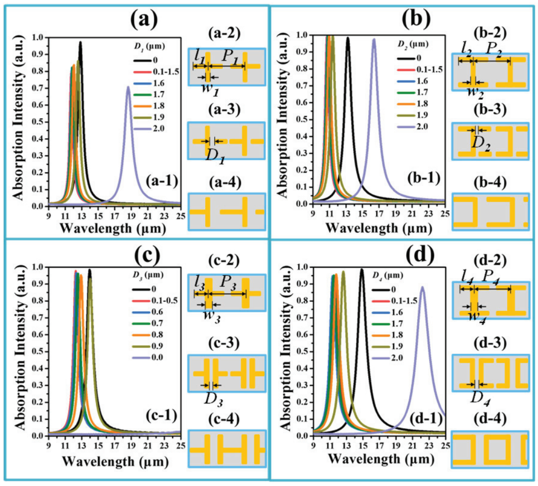

Fig. 3. Absorption intensities of (a-1) IRMA-1, (b-1) IRMA-2, (c-1) IRMA-3, and (d-1) IRMA-4 with different distance between unit cell of top tailored metal layer. Schematics of the unit cells of IRMA-1 with (a-2) $D_1 = 0$ μm, (a-3) $D_1 = 1.0$ μm, and (a-4) $D_1 = 2.0$ μm, IRMA-2 with (b-2) $D_2 = 0$ μm, (b-3) $D_2 = 1.0$ μm, and (b-4) $D_2 = 2.0$ μm, IRMA-3 with (c-2) $D_3 = 0$ μm, (c-3) $D_3 = 0.5$ μm, and (c-4) $D_3 = 1.0$ μm, IRMA-4 with (d-2) $D_4 = 0$ μm, (d-3) $D_4 = 0.5$ μm, and (d-4) $D_4 = 1.0$ μm, respectively. Geometrical dimensions are kept at $l_1 = l_2 = 3.0$ μm, $l_3 = l_4 = 3.5$ μm, $w_1 = w_2 = 1.0$ μm, $w_3 = w_4 = 2.0$ μm, and $P_1 = P_2 = P_3 = P_4 = 8.0$ μm.

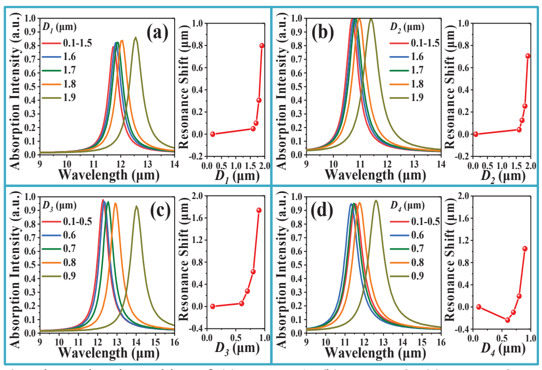

Fig. 4. Absorption intensities of (a) IRMA-1, (b) IRMA-2, (c) IRMA-3, and (d) IRMA-4, respectively. The right images are the corresponding relationships of D_1-D_4 and resonance shifts, respectively.